Lattice QCD

with

Dynamical Domain Wall Fermions

Taku Izubuchi

RIKEN BNL Reserch Center

Kanazawa University

for the Riken-BNL-Columbia collaboration

Introduction

Advantages of Domain Wall Fermions (DWF)
(Kaplan 92, Shamir 93, Furman-Shamir 95)

- Both chiral and flavor symmetry are realized at finite lattice spacings, a, in a good approximation.
- Small O(a) discretization errors : $O(am_{res})$ and $O(a^2 m_f^2)$.
($c.f.$ J. Noaki's talk for quenched simulations.)
- Simple, Continuum-like PQChPT (partially quenched chiral perturbation theory) formulae are presumably applicable for chiral extrapolations on finite lattice spacings.
- No unphysical operator mixing in flavor space, and a very small mixing with wrong chirality operators.
- Positive determinant for positive quark mass (Furman-Shamir) .
$\Longrightarrow \det D = \sqrt{|\det D|^2}$ for odd flavor(s).

DWF is one implementation of Ginsparg-Wilson fermions, which would be the closest lattice fermions to the continuum one.

Plan of this talk

- Introduction
- HMC Evolution Details
- Physical Results
- Conclusion

HMC Evolution Details

As this is the first large-scale study of $N_F = 2$ Dynamical DWF, somewhat detailed description about the ensemble generation may be worth reporting.

To compensate a part of the expense adding the fifth dimension needed for flavor-chiral symmetry , several improvements are made on top of the simulations done by Columbia Univ. (G. Fleming, P. Vranas, $et.al.$) .

- RG improved gauge actions
- Improved fermion force term
- Chronological inverter

The residual chiral symmetry breaking

- From five dimensional Wilson fermion, $\psi(x,s)$, with Wilson mass $-M_5$ (M_5: DWF height),
  the 4-dim quark is picked up from left (right) chirality part at boundaries:

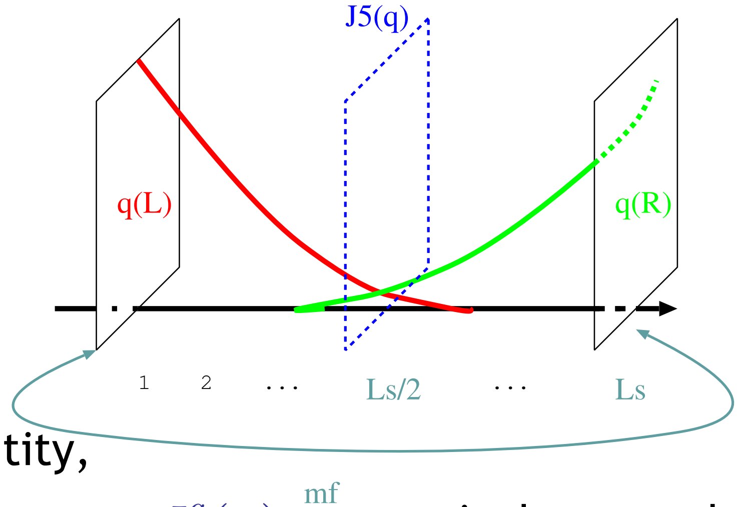

$$q(x) = P_L\psi(x,1) + P_R\psi(x,L_s)$$

$$\bar{q}(x) = \bar{\psi}(x,L_s)P_R + \bar{\psi}(x,1)P_L$$

mass term : $m_f\bar{q}q(x)$

- From the axial Ward-Takahashi identity,

$$\partial_\mu \mathcal{A}^a_\mu(x) = 2m_f J^a_5(x) + 2J^a_{5q}(x)$$
$$\approx 2\,(m_f + m_{res})J^a_5(x)$$

$J^a_5(x)$: non-singlet pseudoscalar,

$J^a_{5q}(x)$: explicit breaking term consists of field at $s = L_s/2 - 1, L_s$.

with the measure of the residual chiral symmetry breaking,

$$m_{res} = \frac{\sum_{x,y}\left\langle J^a_{5q}(y,t)J^a_5(x,0)\right\rangle}{\sum_{x,y}\langle J^a_5(y,t)J^a_5(x,0)\rangle} \quad .$$

m_{res} in quenched simulations

- In practice $L_s \lesssim$ a few 10 is preferable. At the same time am_{res} must be small, less than a few MeV, to realize the advantages of DWF.

- quenched DWF QCD (RBC)

  Wilson gauge action , $a^{-1} \lesssim 2$ *GeV*
  RG improved gauge actions (DBW2, Iwasaki, Symanzik),
  $a^{-1} \simeq 1.3, 2,$ *and 3 GeV.*

for $a^{-1} \approx$ 2 GeV, and $L_s = 16$.

action	m_{res}	am_{res}
Wilson	3 MeV	
Iwasaki	0.3 MeV	
DBW2	0.04 MeV	$1.9(1) \times 10^{-5}$

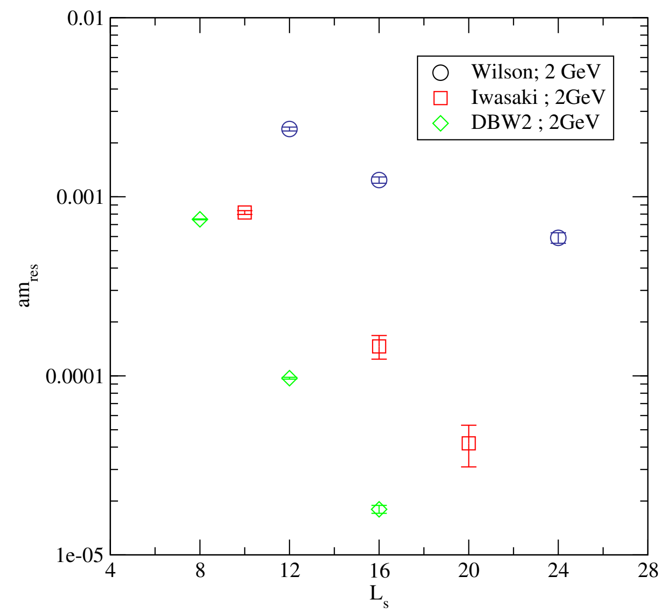

- RG actions reduce m_{res}

- In RG actions, the negative coefficients to the rectangular plaquette suppress dislocations, but the parity broken phase, still exists for small enough β (S. Aoki)
.

Anticipation of m_{res} in the $N_F > 0$ simulations

- To keep the scale obtained from the long-distant physics same, β for the dynamical simulation must be decreased from that of the quenched.

- The gauge field at the short-distance is as rough as that of quenched simulation with same (small) β. (consistent with observations using Schwinger-Dynson technique (C. Dawson))

- m_{res} should be larger than that of quenched simulation.

- In fact,

  $N_f = 2$ *Wilson plaquette action,* $a^{-1} \lesssim 1$ *GeV*
  $\Longrightarrow$ *needs* $L_s \sim 100$ *for small* m_{res}.

- Aiming for $a^{-1} \approx 2$ GeV, we set

DBW2 gauge action with $\beta = 0.80$

by preparatory studies on small lattices, and extrapolations from quenched results.
c.f. quenched DBW2 from m_ρ,

$\beta = 1.04$: $a^{-1} \approx$ *2GeV* .
$\beta = 0.87$: $a^{-1} \approx$ *1.3GeV* .

Simulation parameters

- Lattice size : $16^3 \times 32$
- RG improved gauge actions (DBW2)
- $\beta = 0.80$
- N_F=2 degenerate Dynamical Domain Wall Fermions
- A practical size of the fifth dimension ($L_s = 12$, $M_5 = 1.8$)
- Three dynamical masses: $m_{sea} = 0.02, 0.03, 0.04$

- HMC-Φ algorithm.
- The conjugate momentum is refreshed every $\approx$ 0.5 molecular dynamics (MD) time.
- statistics: $\sim$ 5,000 trajectories

m_{sea}	Δt	Steps/Traj.	Traj.	Acceptance
0.02	$1/100$	51	5361	77%
0.03	$1/100$	51	6195	78%
0.04	$1/80$	41	5605	68%

Acceptance

- Acceptance, $\langle P_{acc}\rangle$, is related to $\Delta H = H_f - H_i$ (the energy difference between the first and the last configuration in a trajectory due to the finite step size in MD, $\Delta t > 0$) :

$$\langle P_{acc}\rangle = \text{erfc}\left(\sqrt{\langle\Delta H\rangle/2}\right) \approx \text{erfc}\left(\sqrt{\langle(\Delta H)^2\rangle/8}\right)$$

- Scaling ansatz (Gupta *et.al.* 90, Takaishi 01) (2nd order integrator):

$$\left\langle(\Delta H)^2\right\rangle = {C_{\Delta H}}^2 V(\Delta t)^4.$$

- By measuring $\left\langle(\Delta H)^2\right\rangle$ (preliminary: standard deviation error)

m_{sea}	Δt	Steps/Trajectory	$\langle P_{acc}\rangle$	$C_{\Delta H}$
0.02	$1/100$	51	77 %	16.2(2)
0.03	$1/100$	51	78 %	15.8(1)
0.04	$1/80$	41	68 %	16.4(2)

- The scaled acceptance, $C_{\Delta H}$, is insensitive to m_{sea} in current parameters, while $C_{\Delta H} \propto m_{sea}^{-\alpha}, \alpha \sim 2$ would be an empirical estimation.

- **Note** These are results for relatively heavy dynamical masses ($m_\pi/m_\rho \sim 0.55 - 0.65$). $C_{\Delta H}$ would likely increase for lighter quark mass.

Improved Force Term

(Vranas, Dawson)

- DWF needs Pauli-Villars field of $m_f = 1$ to cancel off the divergence of the bulk (5-dim) fermions.

$$\Phi_{PV}{}^\dagger [D^\dagger D(m_f = 1)] \Phi_{PV}$$

- Previous works used pseudo fermion field, Φ_F, and Φ_{PV} separately: cancellation was done stochastically $\Longrightarrow$ larger force due to the "mismatch" between Φ_{PV} and Φ_F in a trajectory.

- Improved method uses one pseudo fermion field for both fermion and Pauli-Villars:

$$\begin{aligned}
\frac{\det\left[D^\dagger(m_f) D(m_f)\right]}{\det\left[D^\dagger(1) D(1)\right]} &= \det\left[D^\dagger(m_f) \frac{1}{D(1)} \frac{1}{D^\dagger(1)} D(m_f)\right] \\
&= \int [d\Phi'][d\Phi'^\dagger] e^{-S_{new}} \quad , \\
S_{new} &= \sum_x \Phi'^\dagger D(1) \frac{1}{D(m_f)} \frac{1}{D^\dagger(m_f)} D^\dagger(1) \Phi'
\end{aligned}$$

- Switching to S_{new}, acceptance increases from 56% to 77%, while $C_{\Delta H}$ decreases from 39(4) to 16.2(2) for $m_{sea} = 0.02$.

Chronological Inverter

(Brower, Ivanenko, Levi, Orginos)

In each MD step, we need to solve: $M[U_\mu]\chi = b$.

Forecast solution using past solutions

- Orthogonal basis from previous N_p solutions of CG, (2 Gram-Schmidtś)

$$\{v_n\}_{n=1\cdots N_p}, \qquad v_1 \propto \text{(latest vector)}$$

- Solve linear equation in N_p dim subspace.

$$a_n = G^{-1}_{n,m} b_n,$$

$$G_{n,m} = \langle v_n | M | v_m \rangle, \quad b_n = \langle v_n | b \rangle$$

- use the solution for the CG guess vector

$$\chi_{try} = \sum_{n=1,\cdots,N_p} a_n v_n$$

- overhead: $1 \sim 2 \times N_p^2$ CG count.

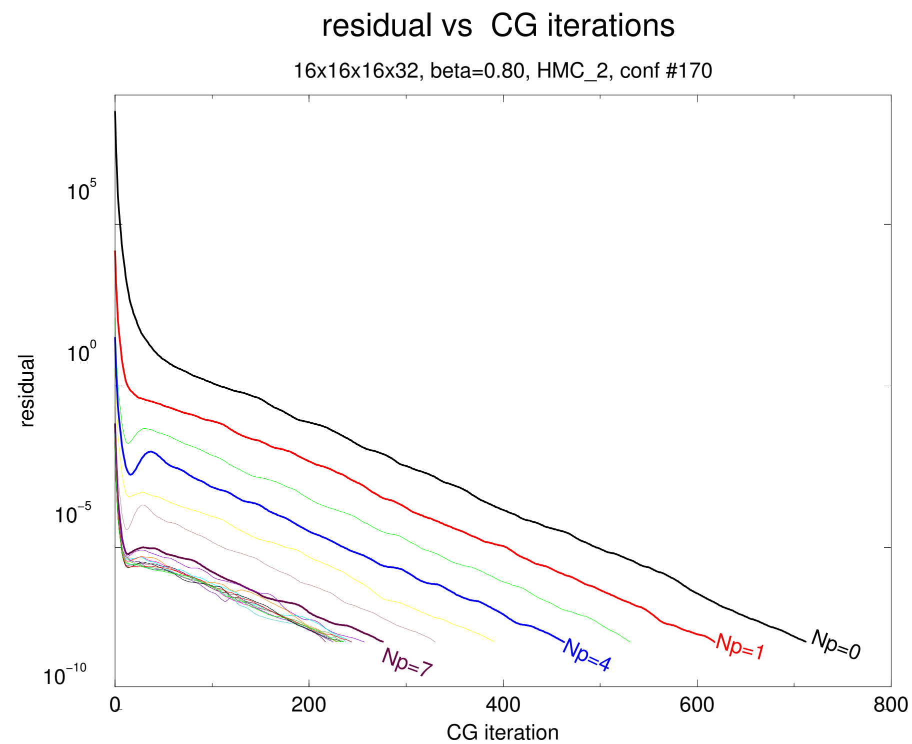

Chronological Inverter...

- $N_{CG}^{(i)}$: average number of matrix multiplication in CG using previous i solution vectors in the forecasting.
  $N_{CG}^{(tot)}$: average total number of multiplication in a trajectory.

- $N^{(i)}$ stop decreasing for $i \gtrsim 7$ for the parameters we use.

m_{sea}	Δt	Steps/Traj.	$N_{CG}^{(0)}$	$N_{CG}^{(7)}$	$N_{CG}^{(tot)}$
0.02	1/100	51	715	277	16,014
0.03	1/100	51	514	158	9,214
0.04	1/80	41	402	121	5,964

- From simple power fits for the three points,

$$N_{CG}^{(i)} = C_i (m_{sea} + m_{res})^{-\beta_i}$$

$\beta_0 \approx 1$, $\beta_7 \approx 1.5$, $\beta_{tot} \approx 1.5$

- Note these numbers would be susceptible to the particular run parameters, especially to Δt.

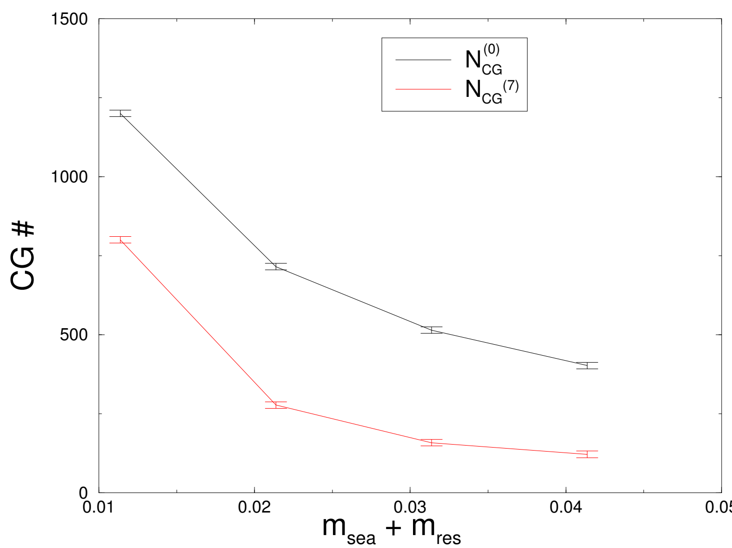

Autocorrelation

$$\rho^{(\mathcal{O})}(t) = \frac{\langle(\mathcal{O}(t) - \langle\mathcal{O}\rangle)(\mathcal{O}(0) - \langle\mathcal{O}\rangle)\rangle}{\langle(\mathcal{O} - \langle\mathcal{O}\rangle)^2\rangle}$$

$$\tau_{int}^{(\mathcal{O})}(t_{max}) = \frac{1}{2} + \sum_{t=1}^{t_{max}} \rho^{(\mathcal{O})}(t)$$

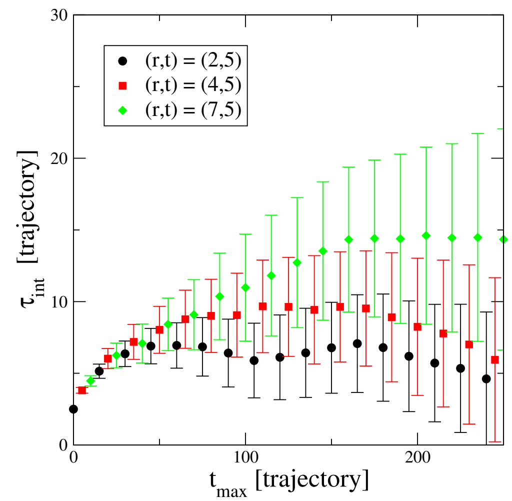

- 1×1 plaquette from $\sim$ 5000 trajectories: $\tau_{int} \lesssim 10$, independent of m_{sea} within jackknife error.

- Smeared Wilson loops, $\langle W(r,t)\rangle$, from every 5 ($m_{sea} = 0.02$) and 10 ($m_{sea} = 0.03, 0.04$) trajectories. APE smear for spacial link.

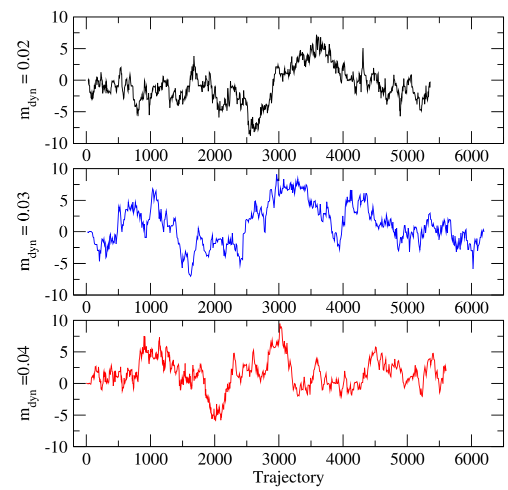

- Axial-Axial, box-point correlator at time-slice 12, from every 10 trajectories, Coulomb gauge fixed box source of size 10, $m_{sea} = 0.02$: $\tau_{int} \approx 40$.

- topological charge. $O(a^2)$ improved definition from clover leafs for 1×1 and 1×2. plaquette.

Summary of the Configuration Generation

- Improved force term increases acceptance.
- The scaled acceptance, $C_{\Delta H}$, is constant in current sea quark mass region.
- The multiple gauge steps (Sexton, Weingarten) would improve performance further.
- Chronological inverter reduces CG count.
- More serious parameter tuning is worth examining in future simulations.

m_{sea}	Steps/Traj.	Traj.	$C_{\Delta H}$	$CG^{(tot)}$	day / 1,000 Traj. (machine)
0.02	51	5361	16.2(2)	16,014	27.3 days (64MB∼200GFLOPS)
0.03	51	6195	15.8(1)	9,214	36.6 days (32MB∼100GFLOPS)
0.04	41	5605	16.4(2)	5,964	29.7 days (32MB∼100GFLOPS)

- Same β, volume but half sea quark mass, $m_{sea} = 0.01$ $(m_\pi/m_\rho \sim 0.4)$, needs roughly 3 months/1,000 Traj. on 64MB (200GFLOPS) QCDSP if acceptance stays same.

Static Quark Potential

- The static quark potential is extracted from Wilson loop, $W(\vec{r},t)$, using APE smear:

$$W(\vec{r},t) = W(\vec{r},0)\ C(\vec{r})\ e^{-V(r)t}$$

The smear parameters are tuned to maximize $C(\vec{r})$: $(c,n) = (0.5, 20)$. For arbitrary $\vec{r}$, all shortest paths are accumulated to increase the number of data points (Bolder *et.al.*) .

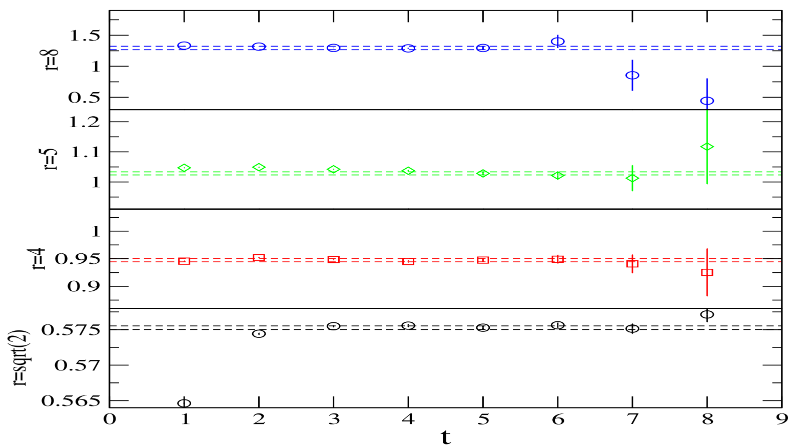

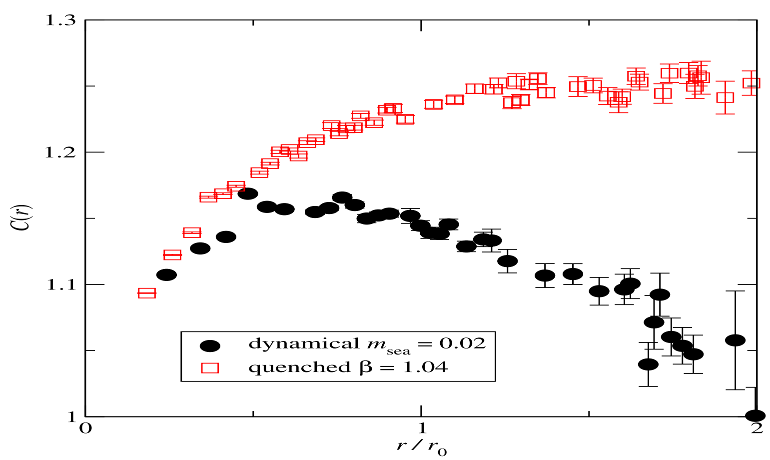

- 941, 559, 473 configurations for $m_{sea} = 0.02, 0.03, 0.04$. Statistical error by the jackknife estimation for block-average over 50 trajectories.

- $V(r)$ has plateau at $t \in [4,6]$.

- $V(r)$ extracted at $[t, t+1]$ approaches to plateau from below for small r. $C(r) > 1$. (Necco)

- $C(r)$ decreases at large r only in dynamical configuration as seen in other dynamical simulations (UKQCD, CP-PACS, SESAM and TχL ...) .

Static Quark Potential ...

$m_{sea} = 0.02, t \in [5, 6]$

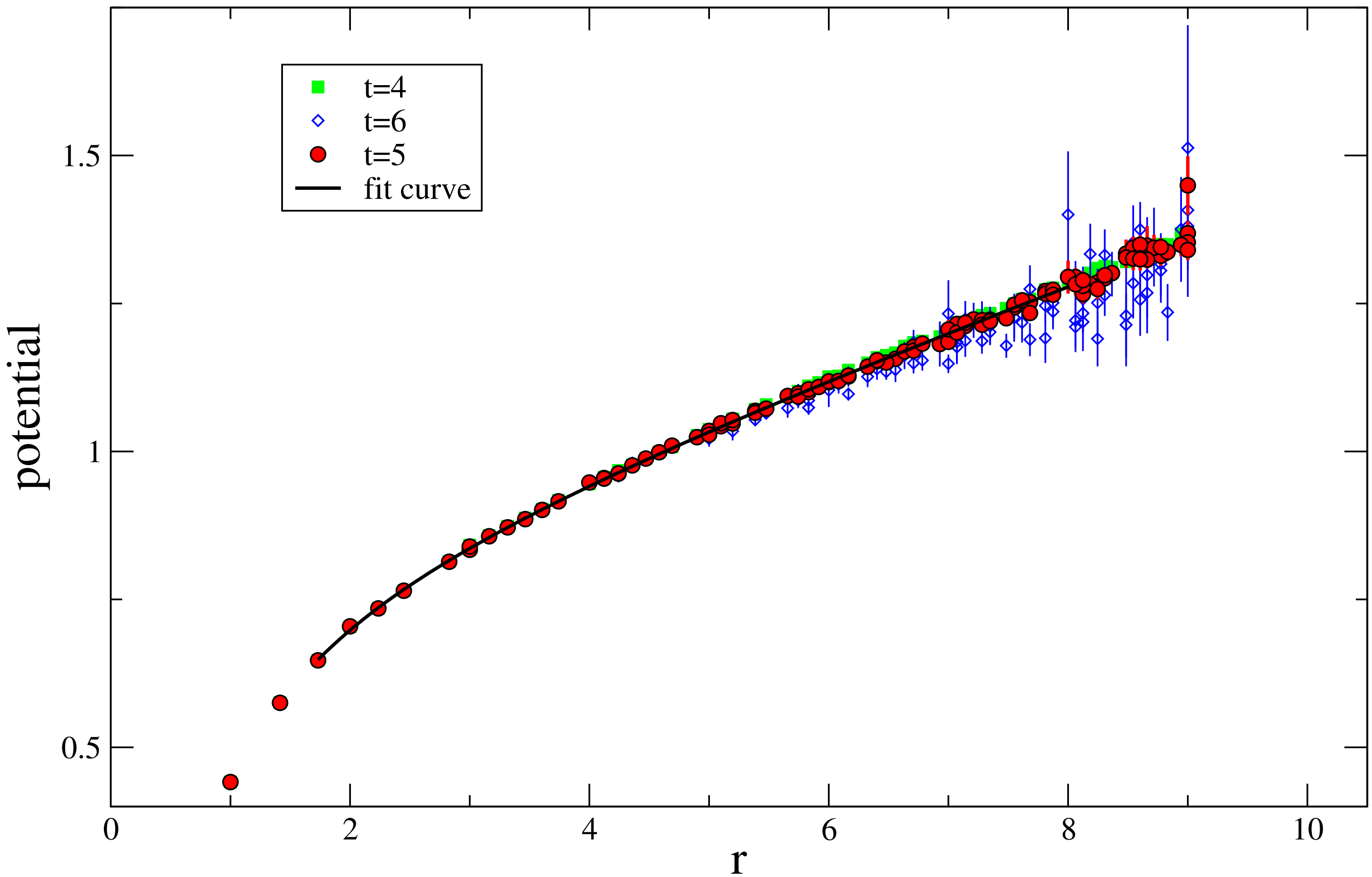

Static Quark Potential ...

analysis: four methods to examine systematic error

$$V(\vec{r}) = V_0 + \frac{\alpha}{r} + \sigma r + l \left[\frac{1}{\vec{r}}\right]_L$$

Sommer scale : $r_0 = \sqrt{\frac{1.65 - \alpha}{\sigma}}$

- $l = 0$ (our main method)
- $l \neq 0, L = \infty$
- $l \neq 0, L = 16$
- Interpolation of (three dimensional) force :

$$|r^2 \nabla V(r_0)| = 1.65$$

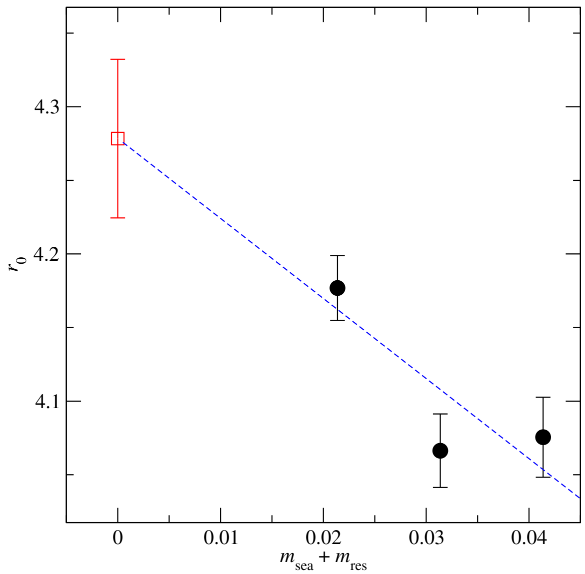

- $V(r)$ extracted $t \in [5, 6]$, then fitted $r \in [\sqrt{3}, 8]$.
- All methods give same r_0 within current statistical error except $l \neq 0, L = 16$ for $m_{sea} = 0.02$.
- Assuming $r_0 = 0.5$ fm,

$$r_0|_{m_{sea} \to -m_{res}} = 4.278(54) \binom{+174}{-011} \quad ,$$

$$a_{r_0}^{-1} = 1.688(21) \binom{+69}{-04} \text{ GeV} \quad .$$

- 9(4)% smaller $m_\rho r_0$ than quenched $\beta = 1.04$

Hadron spectrum and decay constants

- chiral limit: $m_f = -m_{res}$
- Hadron made of degenerate valence quarks (except B_K).
- Coulomb gauge fixed wall source point sink for hadron masses, and non-gauge-fixed wall-point (Kuramashi wall) for decay constant.
- 94 configurations from every 50 trajectories for each m_{sea} leaving first $\sim$ 600 configurations for thermalization.
- Chiral extrapolation:
  - *observables in lattice unit are extrapolated.*
  - *Linear functions of m_{sea}, m_{val}.*
  - *The next-to leading order partially quenched chiral perturbation theory formulae (NLO).*

m_{res}

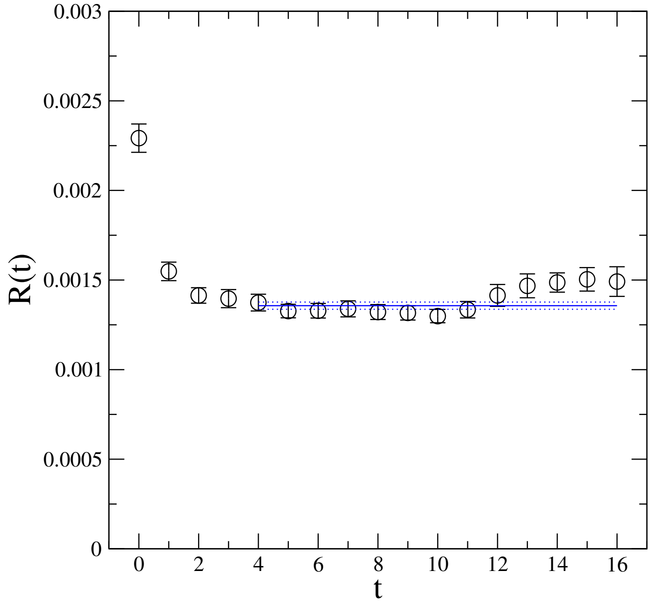

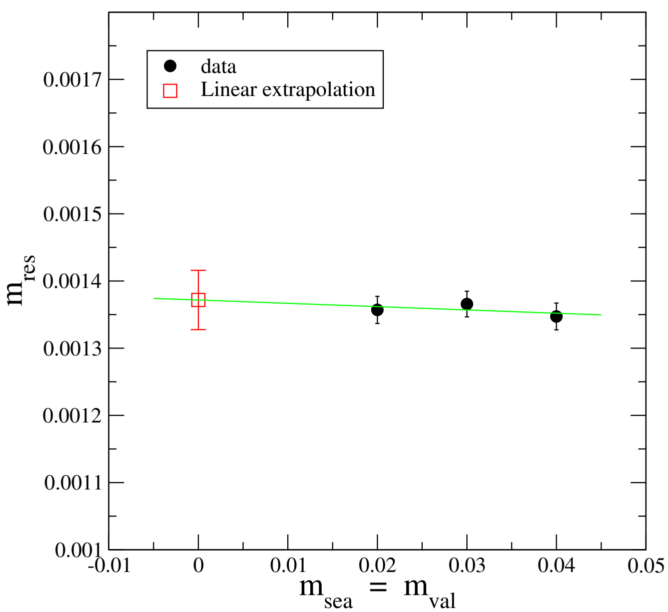

- Wall-point correlator,

$$R(t) = \frac{\langle J_{5q}(t) J_5(0) \rangle}{\langle J_5(t) J_5(0) \rangle}$$

- constant fit at $t \in [4, 16]$.
- The quark mass dependence is very weak.
- Chiral limit is defined as

$$m_f = m_{res}|_{m\to 0} = 0.001372(44)$$

- Larger than quenched DBW2 ($\beta = 1.04$) value for same $L_s = 12$.
- An order of magnitude smaller than input quark mass, under control.

Pseudoscalar decay constant

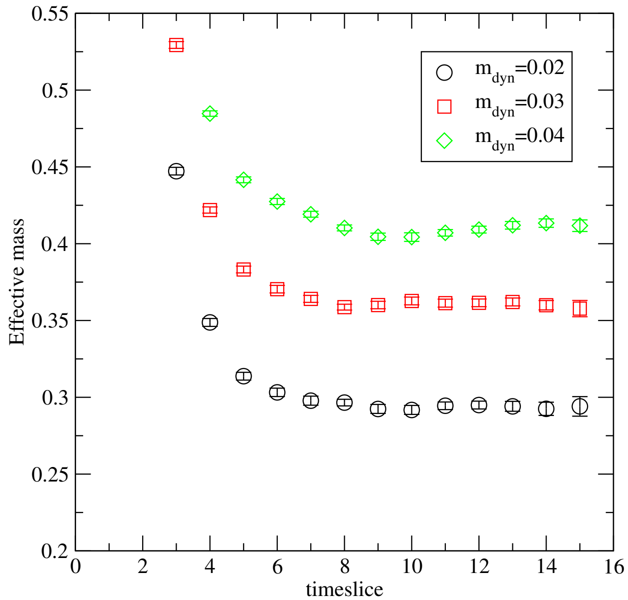

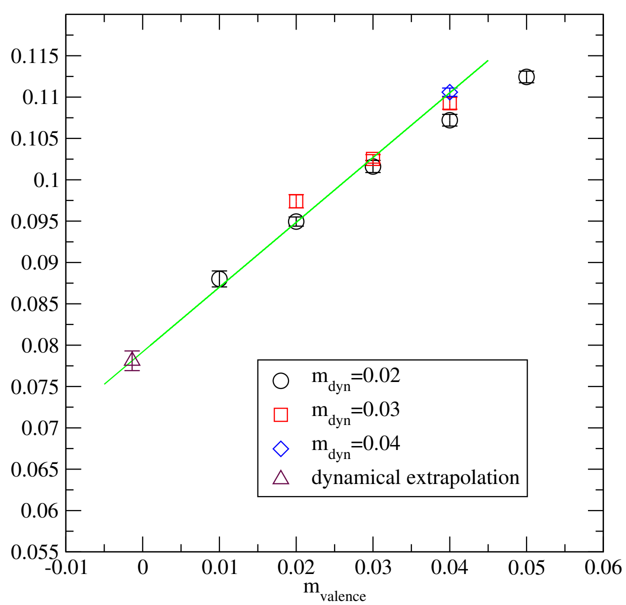

- un-gauge-fixed wall source point sink pseudoscalar correlator $\langle J_5 J_5 \rangle$.
-

$$\langle 0|J_5|PS\rangle = f_{PS}\frac{M_{PS}^2}{2(m_{val}+m_{res})},$$

$$\langle 0|A_4|PS\rangle = f_{PS}^{lat} M_{PS} = \frac{f_{PS}}{Z_A} M_{PS},$$

- $\langle A_4 A_4 \rangle$ has larger statistical error for mass, but consistent with $\langle J_5^a, J_5^a \rangle$.
- linear fit for $m_{val}, m_{sea} \in [0.01, 0.04]$:

$$f_{PS} = f + c_1 \frac{m_1 + m_2}{2} + c_2 m_{sea}$$

$$f = 0.0781(14)$$

Pseudoscalar decay constant...

- NLO fits are also examined.
- $m_{val}, m_{sea} \in [0.01, 0.03]$
- 30% smaller f than linear fit.
- Larger mass points are missed badly.

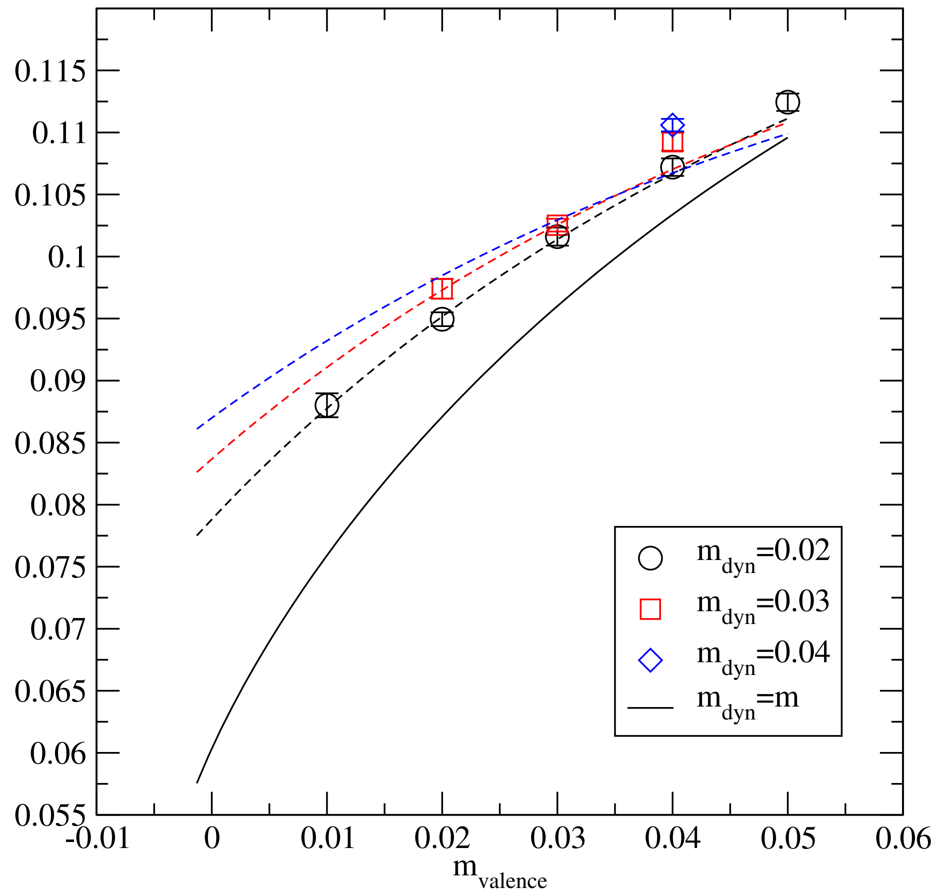

vector meson mass

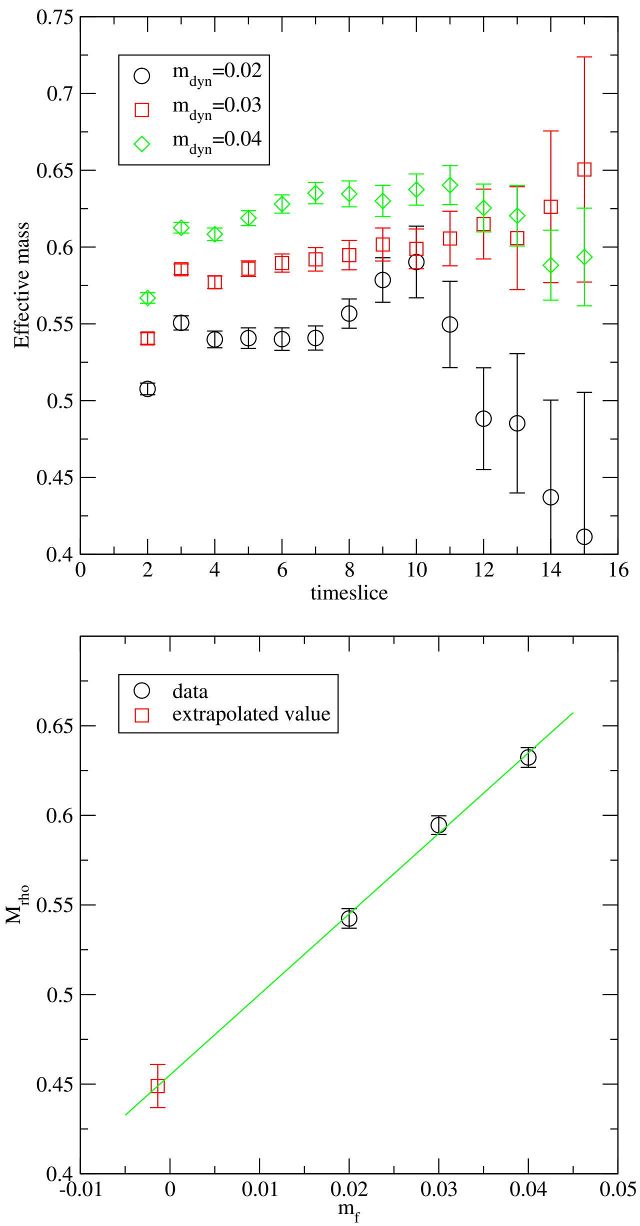

- Wall-point correlator.
- Relatively poor plateau.
- $t \in [t_{min}, 16]$, $t_{min} = 5, 6, 7$ for $m_{sea} = 0.02, 0.03, 0.04$.
- From m_π / m_ρ by a linear fit + NLO fit for m_{ps},

$$a^{-1} = 1.690(53)\text{GeV} \quad ,$$

($c.f.$ $a_{r_0}^{-1} = 1.688(21) \left({}^{+69}_{-04}\right)$.)

- At dynamical points:
  $m_{ps}/m_v = 0.536(7), 0.600(6), 0.647(6)$
  or
  $m_{ps} \approx \frac{1}{2}, \frac{3}{4}, 1 \times m_{strange}$

pseudoscalar meson mass

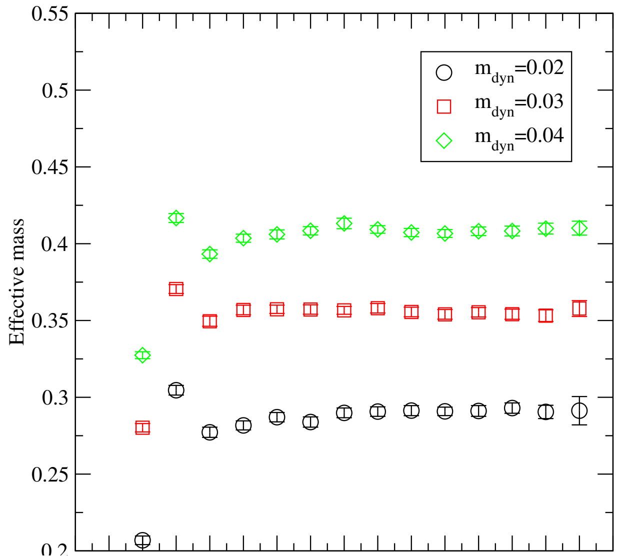

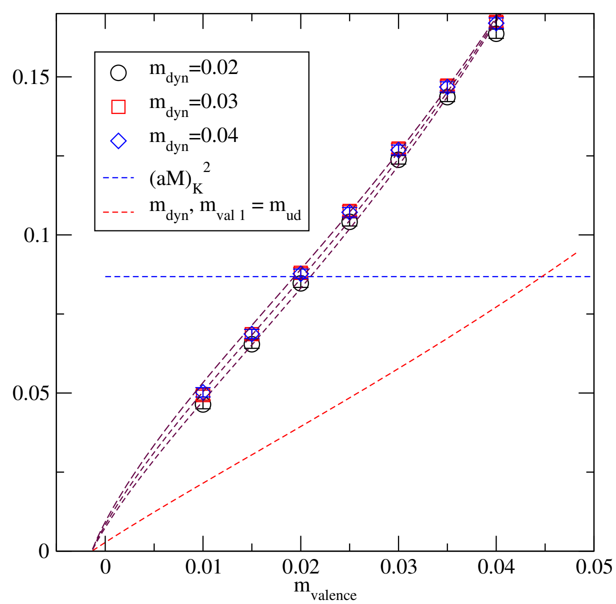

- Wall-point correlator $\langle A_4 A_4 \rangle$ and $\langle J_5 J_5 \rangle$.

- Smaller statistical error for $\langle A_4 A_4 \rangle$. Masses are extracted from $t \in [9, 16]$.

- A linear extrapolation m_{ps}^2 to $m_f = -m_{res}$ is zero. $m_{ps}^2 = 0$ at $m_f \approx -(2-3) \times m_{res}$ in quenched simulation. $\longrightarrow$ Consistent with (quenched) chiral logarithms $(m_{ps}^2/m \sim 2B_0 + cm \log m)$ vs $(m_{ps}^2/m \sim \log m)$.

- NLO fit for $m_{sea,val} \in [0.01, 0.04]$ is not inconsistent.

Pseudoscalar Meson mass ...

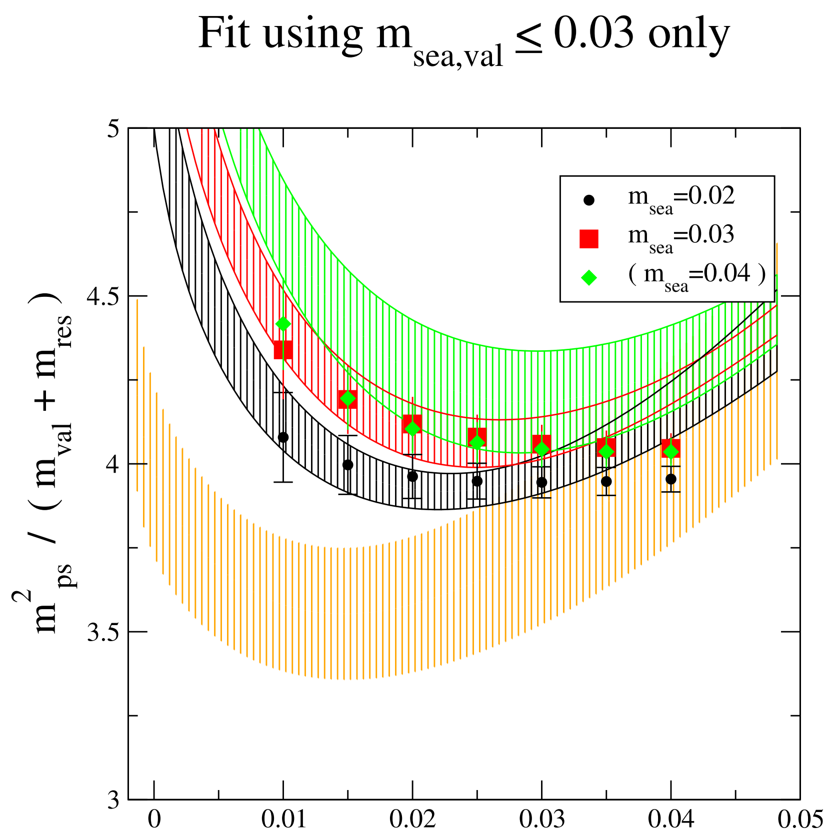

- NLO fit using $m_{sea,val} \leq 0.03$
- constraints:
  - $m^2_{ps} = 0$ at $m_{val,sea} = -m_{res}$,
  - $f = 0.0781$ from linear fit of f_{ps}.
- From neutral pion mass

$$\bar{m} = 2.4(15) \times 10^{-4}$$

- Using NLO for non-degenerate valence quark with same low energy constants : $m_{strange} = 0.0447(25)$
- renormalized quark mass : $m^{\bar{M}S} = (m + m_{res})/Z_s$, $Z_s \sim 0.6$ (Dawson Lattice2003) .
-

Other Physical Results (preliminary)

- NLO fits results using m_{ps}^2 at $m_f = m_{sea,val} \leq m_f^{(max)}$. Pseudo-scalar wall-point (upper two column), and axial-vector wall point. uncorrelated χ^2. Gasser-Leutwyler low energy constants L_i multiplied by 10^4 at $\Lambda_\chi = 1$ GeV.

$m_f^{(max)}$	χ^2/dof	$2\,B_0$	$L_4 - 2L_6$	$L_5 - 2L_8$
0.03	$0.1(1)$	$4.0(3)$	$-1.5(7)$	$-2(1)$
0.04	$2(1)$	$4.2(1)$	$-0.2(4)$	$-1.1(4)$
0.03	$0.3(2)$	$4.0(3)$	$-1.9(8)$	$-1(1)$
0.04	$1.9(9)$	$4.2(1)$	$-0.4(4)$	$-0.8(3)$

- By linear extrapolations/interpolations for f_{ps} to $\bar{m}$ and m_s,

	$N_F = 2$	experiment	$N_F = 0$
f_π	134(4)	130.7	129.0(50)
f_K	157(4)	160	149.7(36)
f_K/f_π	1.18(1)	1.224	1.118(25)

better agreement with experiment than quenched DWF simulations.

Other Physical Results (preliminary)...

- $$J = m_V \left. \frac{dm_{ps}^2}{dm_V} \right|_{m_V/m_{ps}=1.8}$$

m_{sea}	$-m_{res}$	0.02	0.03	0.04	quenched $\beta = 1.04$
J	0.461(61)	0.408(19)	0.393(25)	0.349(50)	0.387(16)

  closer value to the phenomenological estimation 0.48(2).

- Baryon mass :

  $$\frac{m_N}{m_\rho} = 1.34(4)$$

  larger than experimental value, and consistent with quenched results for $m_{sea,val} \in [0.02, 0.04]$. The sea quark effect is hardly seen in current statistics.

conclusion

- We have generated ensembles of Lattice QCD with $N_F = 2$ dynamical DWF
  - three m_{sea}: 0.02, 0.03, 0.04
  corresponding to $m_{ps}/m_V = 0.54(1), 0.60(1), 0.65(1)$ or
  $m_{ps} \approx \frac{1}{2}, \frac{3}{4}, 1 \times m_{strange}$,
  - Statistics: $\sim$ 5,000 trajectories ,
  - Lattice spacing: $a^{-1} = 1.690(53)$ GeV ,
  - Volume: $V \approx (1.9\text{fm})^3$,
  - $m_{res} = 0.001372(44) \lesssim$ 5 MeV

- The NLO fit to m_{ps}^2 is not inconsistent.

- NLO formula did not describe the data of f_{ps}.

- Comparing to $N_F = 0$ DWF, closer agreements with experimental value are found.

Exploratory results of $N_F = 3$

- $16^3 \times 32$, DBW2, $\beta = 0.72$, $m_{sea} = 0.04, L_s = 8$ 1,500 trajectories generaged using HMC-R ($\Delta t = 0.01$)
  $\Longrightarrow$ $m_{res} = 0.017(1)$, $a^{-1} \approx 1.6 - 1.7$ GeV at chiral limit using m_V, r_0.

- m_{res} as a function of valence L_s (M. Lin, Mawhinney)

$m_{\rm res}$ **versus** L_s **for** $N_f = 0, 2$ **and 3**

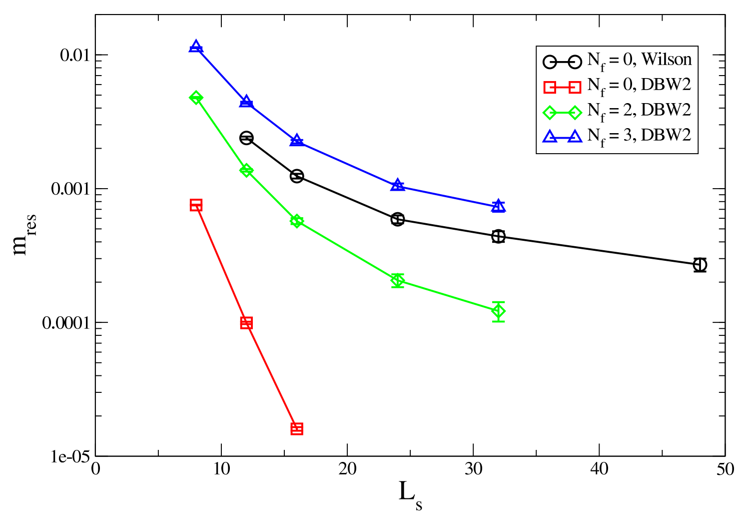

- RHMC is implemented in CPS (Clark) .